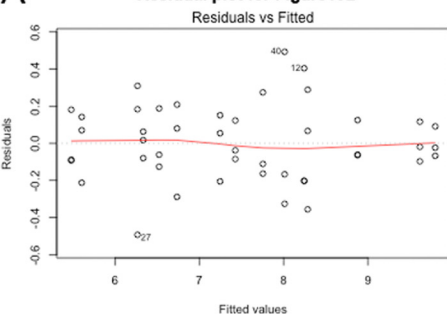
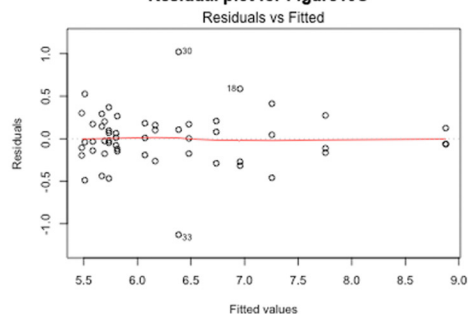


A

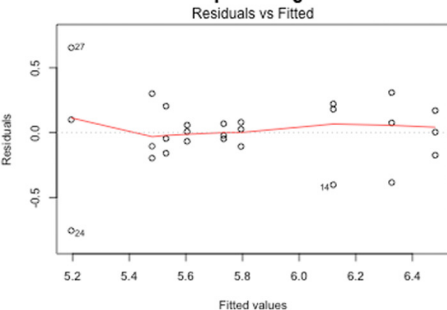
Residual plot for Figure10B



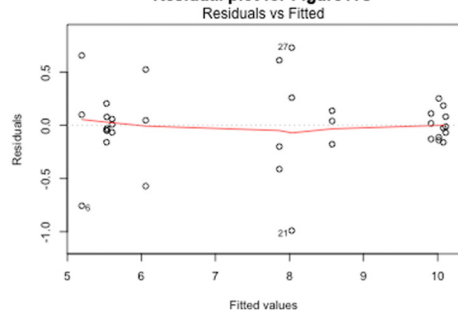
Residual plot for Figure10C



Residual plot for Figure11B

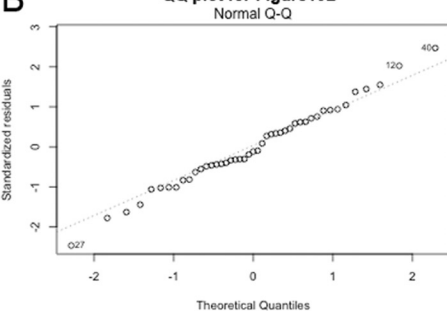


Residual plot for Figure11C

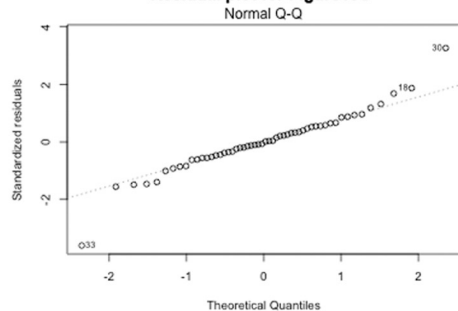


B

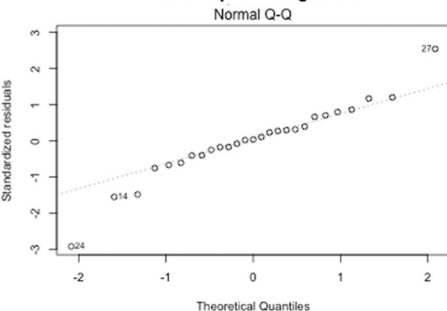
QQ plot for Figure10B



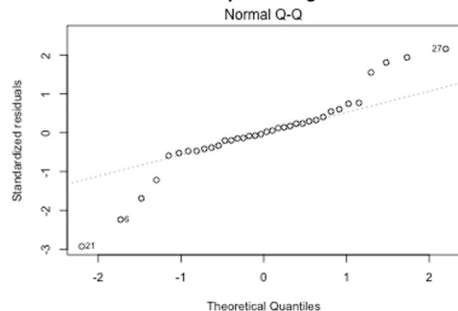
Residual plot for Figure10C



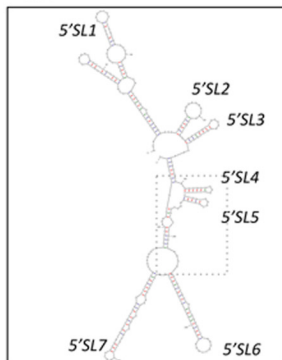
Residual plot for Figure11B



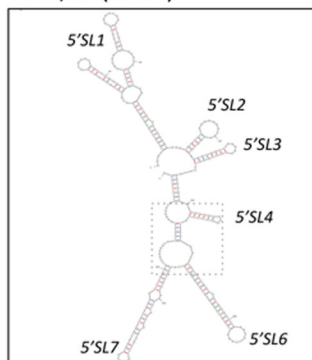
Residual plot for Figure11C



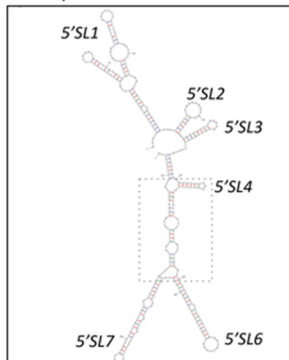
C68



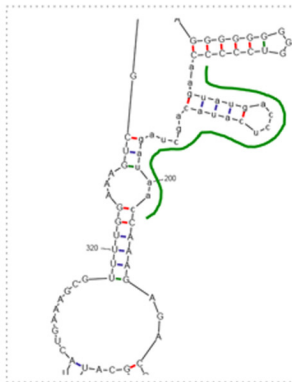
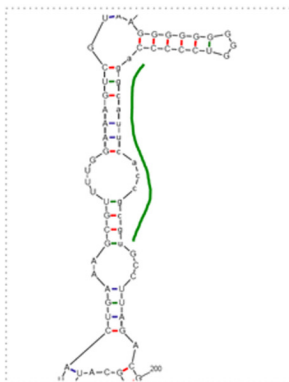
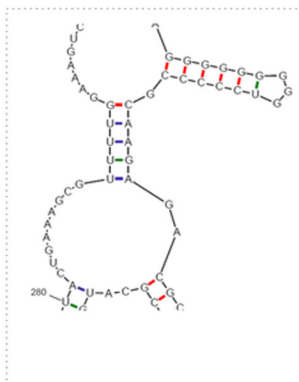
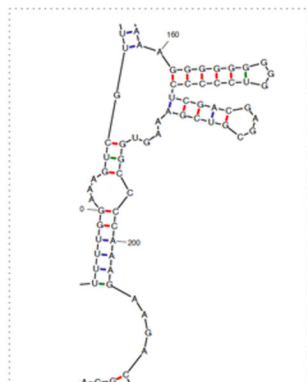
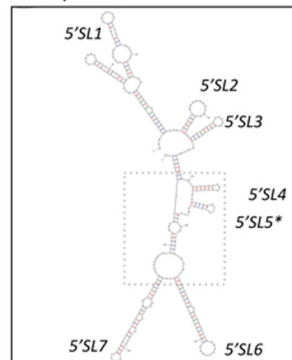
C68/del(15-24)



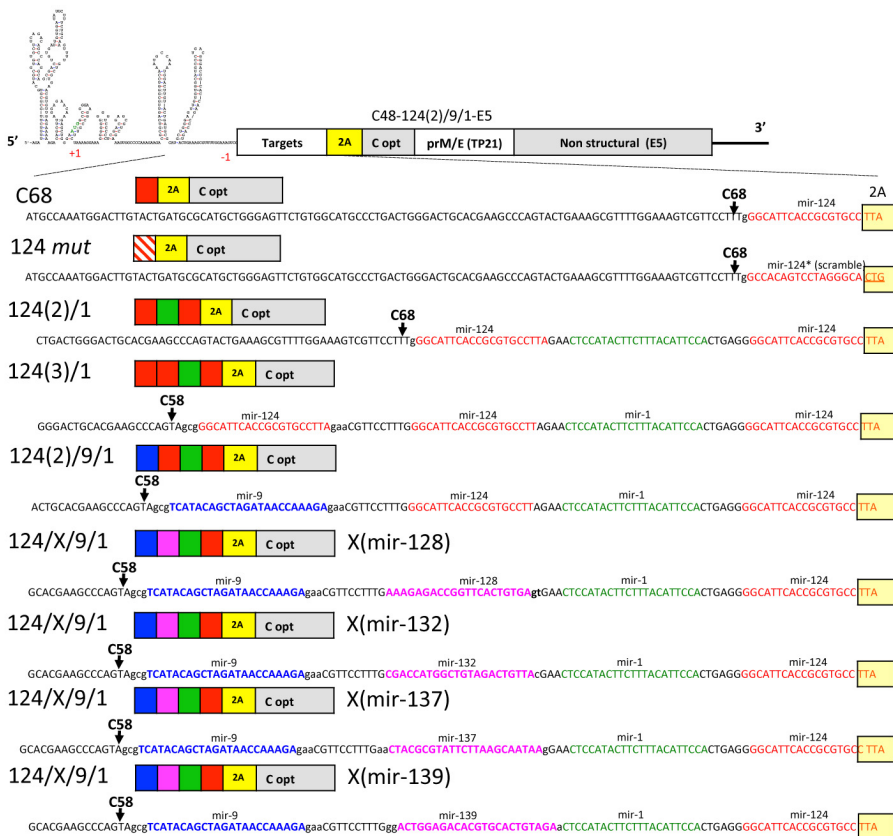
C68/int15



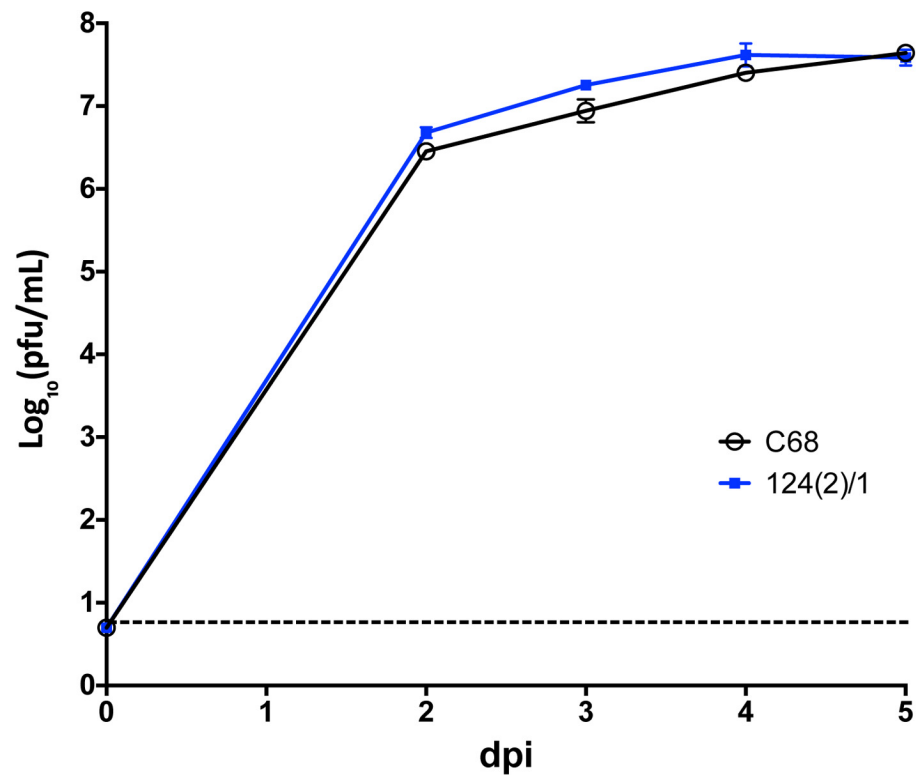
C68/int27



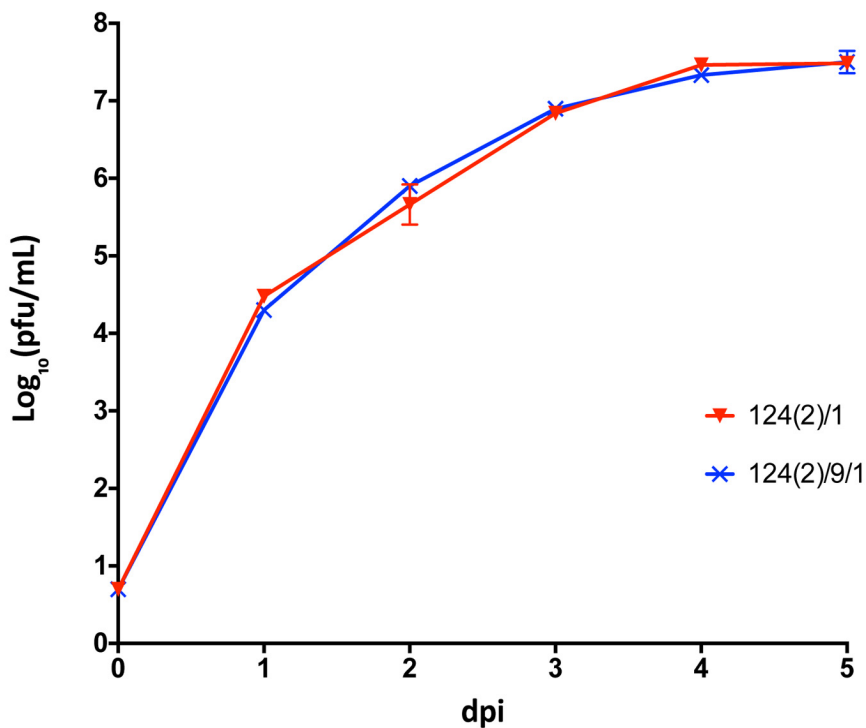
Supplementary Figure S2



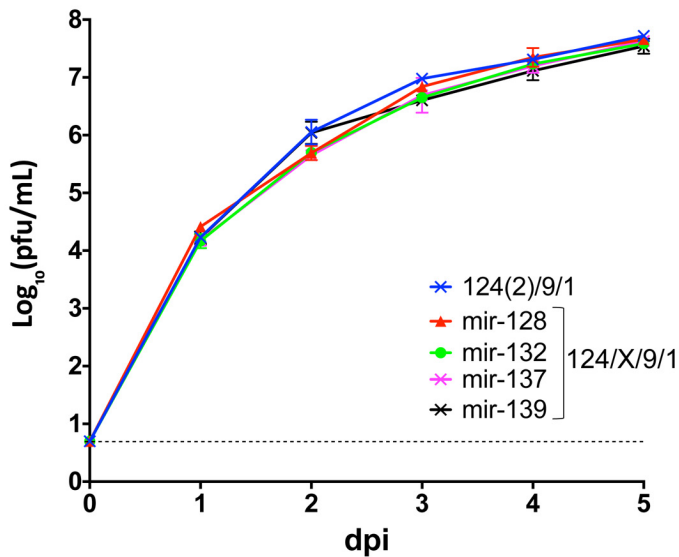
Supplementary Figure S3



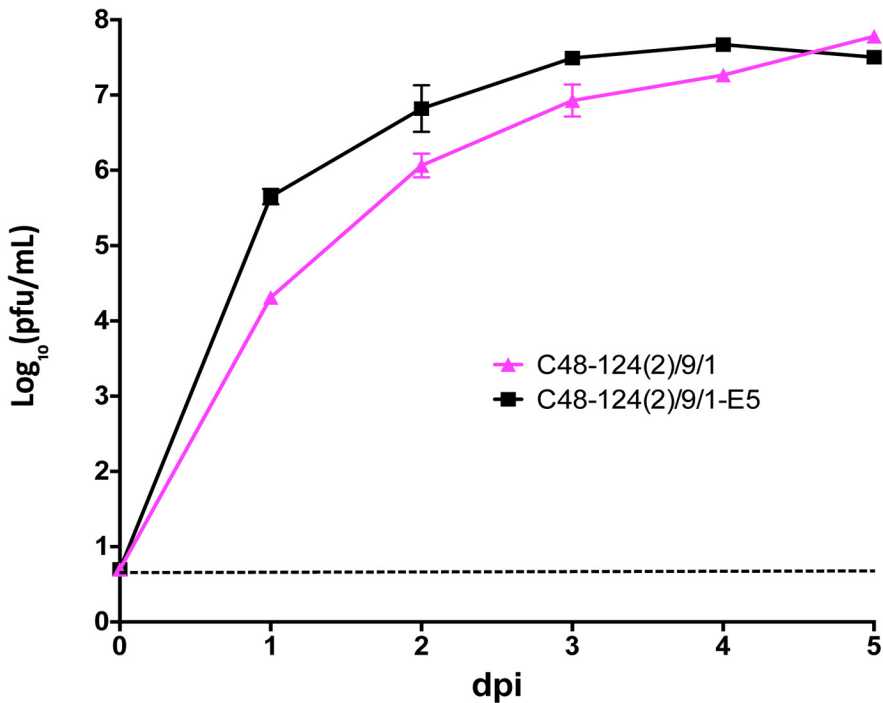
Supplementary Figure S4



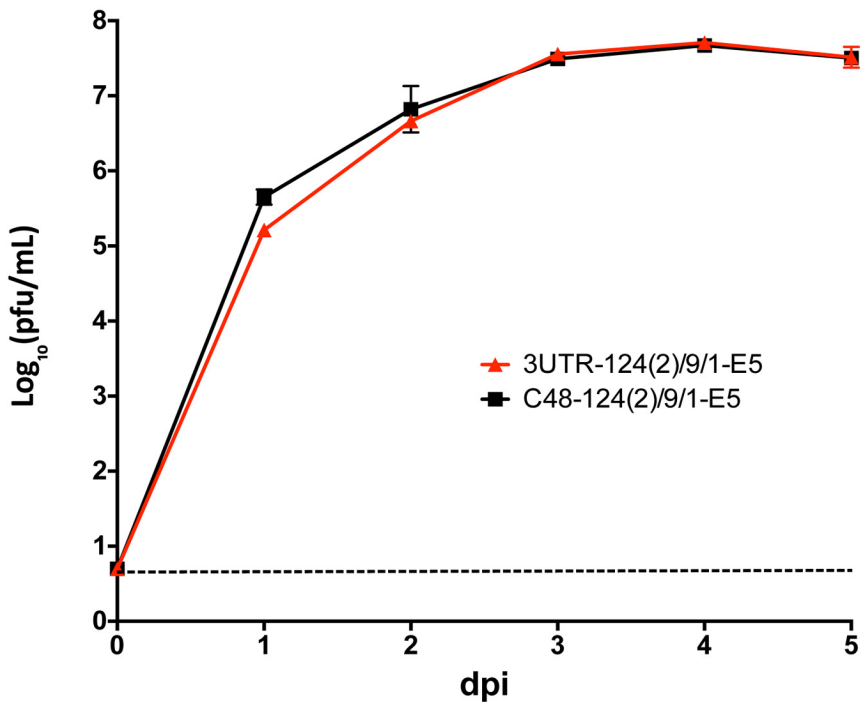
Supplementary Figure S5



Supplementary Figure S6

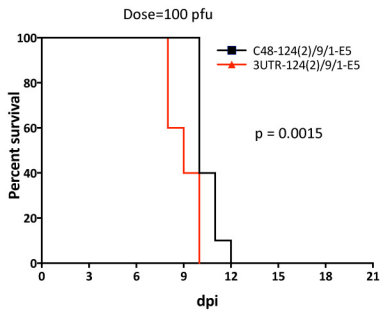


Supplementary Figure S7

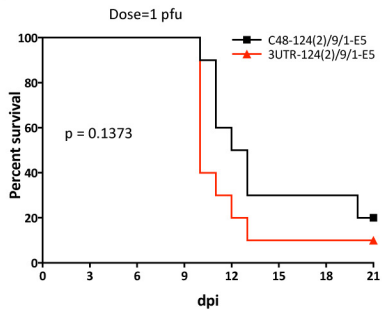


Supplementary Figure S8

A

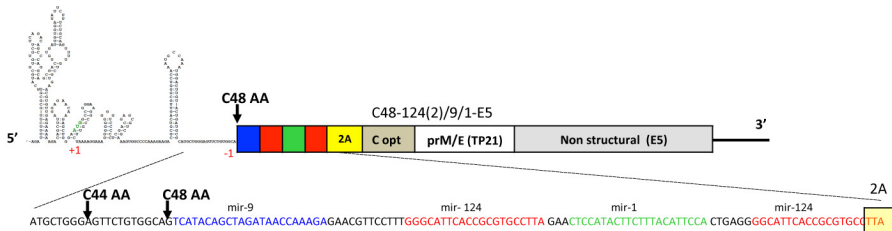


B

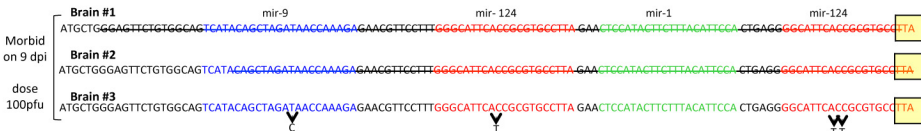


Supplementary Figure S9

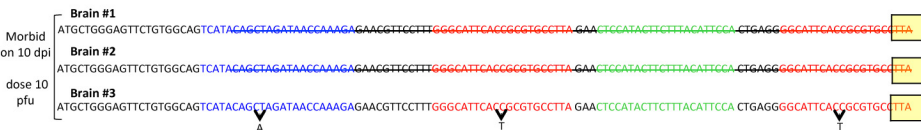
A



B



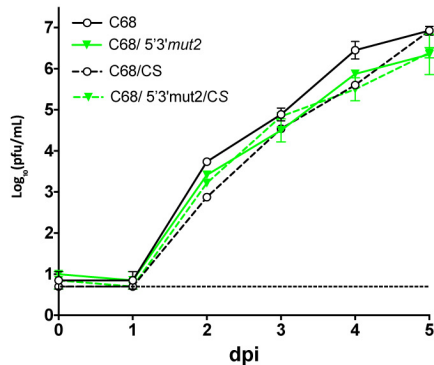
C



Supplementary Figure S10

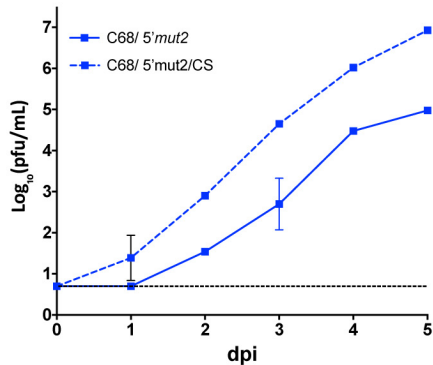
A

Kissing +



B

Kissing -



Supplementary Figure S11

Supplementary Figures legends

Supplementary Figure S1. The scatter plots for residuals (A) and quantile-quantile plots for residuals (B) calculated from ANOVA models presented in Figures 10 and 11.

Supplementary Figure S2. Predicted secondary RNA structure of the 5' terminal regions of C68, C68/del(15-24), C68/int15, and C68/int27 viruses.

Structures were generated using m-fold web server for nucleic acid folding (<http://mfold.rna.albany.edu/?q=mfold>) with default parameters. Inserted 15 and 27 nt sequences are indicated by the green lines.

Supplementary Figure S3. Detailed sequence (cDNA) of miRNA targeting region for viruses depicted in Figure 10.

Supplementary Figure S4. Growth kinetics of C68 and 124(2)/1 viruses in Vero cells.

Vero cells monolayers in T25 flasks were transfected with 5 µg of indicated DNA constructs. Virus aliquots in cell culture medium were collected for each indicated time point and titrated in Vero cells in duplicate. Mean virus titers ± SD are shown. The dashed line indicates the limit of virus detection ($0.7 \log_{10}$ pfu/mL).

Supplementary Figure S5. Effect of insertion of target sequence for mir-9 into the DCGR on LGTV growth in Vero cells.

Vero cells were transfected with 5 µg of plasmid DNA. Samples were collected daily for 5 days. Individual samples for each time point were titrated in Vero cells in duplicate and results were presented as an average ± standard deviation (shown as brackets).

Supplementary Figure S6. Effect of mir-124 target sequence substitution with a target for mir-128, mir-132, mir-137, or mir-139 in the 124(2)/9/1 genome on virus growth in Vero cells.

A target sequence for mir-128, mir-132, mir-137, or mir-139 was used to replace a 5' terminal copy of mir-124 target sequence in 124(2)/9/1 construct (**Figure 10**). Vero cells

were transfected with 5 µg of each of plasmid DNAs. Virus aliquots in cell culture medium were collected for each indicated time point, and virus titers (\pm SD) were determined in Vero cells in duplicate.

Supplementary Figure S7. Effect of amino acid substitutions in non-structural proteins of C48-124(2)/9/1 with corresponding sequence derived from LGTV E5 strain on growth kinetics of resulting virus (C48-124(2)/9/1-E5) in Vero cells.

Vero cells were transfected with 5 µg of plasmid DNA. Virus aliquots in cell culture medium were collected for each indicated time point, and virus titers (\pm SD) were determined in Vero cells in duplicate.

Supplementary Figure S8. Insertion of targets for mir-124, mir-9 and mir-1 in the 3'NCR does not increase virus production in Vero cells compared to that of viruses carrying these miRNA targets in the DCGR.

A set of miRNA targets for mir-124, mir-9 and mir-1 was inserted in the 3'NCR of chimeric LGTV TP-21/E5 virus genome to generate 3UTR-124(2)/9/1-E5 construct (**Fig. 11A**). Vero cells were transfected with 5 µg of C48-124(2)/9/1-E5 or 3UTR-124(2)/9/1-E5 DNA constructs. Virus aliquots in cell culture medium were collected for each indicated time point, and virus titers (\pm SD) were determined in Vero cells in duplicate.

Supplementary Figure S9. Insertion of miRNA target sequences for brain-specific miRNA into DCGR results in increased survival of newborn mice compared with target insertion into 3'NCR.

Litters of 10 suckling mice were infected IC with 100 pfu (**A**) or 1 pfu (**B**) of C48-124(2)/9/1-E5 or 3UTR-124(2)/9/1-E5 virus and monitored daily for morbidity for 21 days. Differences in mice survival were compared using log-rank (Mantel-Cox) test implemented in Prism 6 software.

Supplementary Figure S10. Genetic stability of miRNA targets in the DCGR of LGTV in mice.

(A) Schematic representation of C48-124(2)/9/1 genome and sequence of the miRNA targets inserted between C48 AA promoter and 2A protease gene. (B and C) Location of point nt mutations and size of the deletions (strikethrough lines) in the escape mutants accumulated in the brains of suckling mice infected IC with 1 or 100 PFU of miRNA-targeted C48-124(2)/9/1 virus. Brains of suckling mice that succumbed to infection on day 9 or 10 p.i. were harvested, and virus RNA was isolated from the brain homogenate for the sequence analysis.

Supplementary Figure S11. Effect of U→C substitution (CS) on growth of viruses with (A) unmodified (C68) or restored (C68/5'3'mut2) kissing-loop contact, or (B) impaired (C68/5'mut2) kissing-loop contact in tick-derived cells.

Confluent monolayers of tick ISE6 cells derived from *Ixodes scapularis* (1) were infected in duplicate with recombinant LGTV with (solid lines) or without (dashed lines) U→C substitution (CS) at an MOI of 0.01. Each time point represents the mean \pm SD of two replicates. Cells were maintained at 34°C in 66% Leibovitz's L-15 medium (Invitrogen) supplemented with 3.3% FBS (Lonza), 6.6% Tryptose phosphate broth solution (MP Biomedicals, Irvine, CA), 0.66 % bovine cholesterol lipoprotein concentrate (MP Biomedicals, Irvine, CA), 50 μ g/ml of gentamicin (Invitrogen), 0.296 g/L of L-aspartic acid, 0.333 g/L of L-glutamine, 0.3 g/L of L-proline, 0.323 g/L of L-glutamic acid, 0.296 g/L of α -ketoglutaric acid, 11.9 g/L of D-glucose, and with 1x mineral and vitamin solutions that have been described earlier (2). The dashed line indicates the limit of virus detection (0.7 log₁₀ pfu/mL).

References:

1. Munderloh, U.G., Liu, Y., Wang, M., Chen, C. and Kurtti, T.J. (1994) Establishment, maintenance and description of cell lines from the tick *Ixodes scapularis*. *The Journal of parasitology*, **80**, 533-543.
2. Munderloh, U.G. and Kurtti, T.J. (1989) Formulation of medium for tick cell culture. *Experimental & applied acarology*, **7**, 219-229.

Supplementary Table S1 Summary of miRNA target sequences used in the study.

miRNA Target	Sequences 5'→3' ^a	Color code used in the paper	Specificity	Length (nt.)
mir-124	GGCATTACCGCGTGCCTTA	Red / solid	brain	20
mir-124*	GcCAcaGtCCtaGgGCacTg	Red / stripes	none	20
mir-9	TCATACAGCTAGATAACCAAAGA	Blue / solid	brain	23
mir-9*	TgATcCAatTgGAcAAtCagAGg	Blue / stripes	none	23
mir-1	CTCCATACTTCTTTACATTCCA	Green / solid	tick	22
mir-1*	tTgCAcACgagccTtCAcagtA	Green / stripes	none	22
mir-128	AAAGAGACCGGTTCACTGTGA	Magenta / solid	brain	21
mir-132	CGACCATGGCTGTAGACTGTTA	Magenta / solid	brain	22
mir-137	CTACGCGTATTCTTAAGCAATAA	Magenta / solid	brain	23
mir-139	ACTGGAGACACGTGCACTGTAGA	Magenta / solid	brain	23

^a Lowercase letters indicate synonymous mutations that were incorporated to alter nucleotide sequence of target miRNA region in control viruses.